Full Length Research Paper

Evaluation of thermodynamic properties of ammonia-water mixture up to 100 bar for power application systems

N. Shankar Ganesh* and T. Srinivas

Vellore Institute of Technology, Vellore-632014, India.

In Kalina power generation, as well as vapor absorption and refrigeration systems ammonia-water mixture has been used as working fluids. In this work, new MatLab code was developed to calculate the thermodynamic properties which will be used to simulate Kalina cycle. The progam developed in MatLab gives fast calculation of the thermodynamic properties. The correlations proposed by Ziegler and Trepp (1984), Patek and Klomfar (1995) and Soleimani (2007) were used to calculate the property diagrams in MatLab. The solved properties are bubble point temperature, dew point temperature, specific enthalpy, specific entropy, specific volume and exergy. A flowchart was developed to understand the computation of the properties. The property chart that is enthalpy-concentration, entropy-concentration, temperature-concentration and exergy-concentration charts have been prepared. The present work can be used to simulate the power generating systems to get the feasibility of the proposed ideas up to 100 bar. This work can be used to carry out the exergy analysis of Kalina power cycles.

Key words: Ammonia-water mixture, thermodynamic, power generation.

BACKGROUND

In ammonia-water mixture, ammonia has got low boiling point which makes it useful for utilizing the waste heat source and makes the possibility of boiling at low temperature. Ammonia-water mixture as non-azeotropic (for a non-azeotropic mixture, the temperature and composition continuously change during boiling) nature will have the tendency to boil and condense at a range of temperatures which possess a closer match between heat source and working fluid mixture. As ammonia have got a similar molecular weight as that of water, it makes it possible to utilize the standard steam turbine components.

For determining the thermodynamic properties of ammonia-water mixtures, various studies were published.

Ziegler and Trepp (1984) described an equation for the thermodynamic properties of ammonia-water mixture in absorption units. In his work, the Gibbs excess energy equation was utilized for determining the specific enthalpy, specific entropy and specific volume. They developed the properties up to a pressure of 50 bar and temperature of 500 K. Barhoumi et al. (2004) presents modelling of the thermodynamic properties. Feng and Yogi (1999) combine the Gibbs free energy method for mixture properties and the bubble and dew point temperature equations for phase equilibrium were used. Patek and Klomfar (1995) give a fast calculation of thermodynamic properties. Senthil and Subbarao (2008) present fast calculation for determining enthalpy and entropy of the mixtures.

The main objectives of the present work are to combine correlations proposed by Ziegler et al. (1984) and carried out in MatLab, which avoids numerous procedure and

---

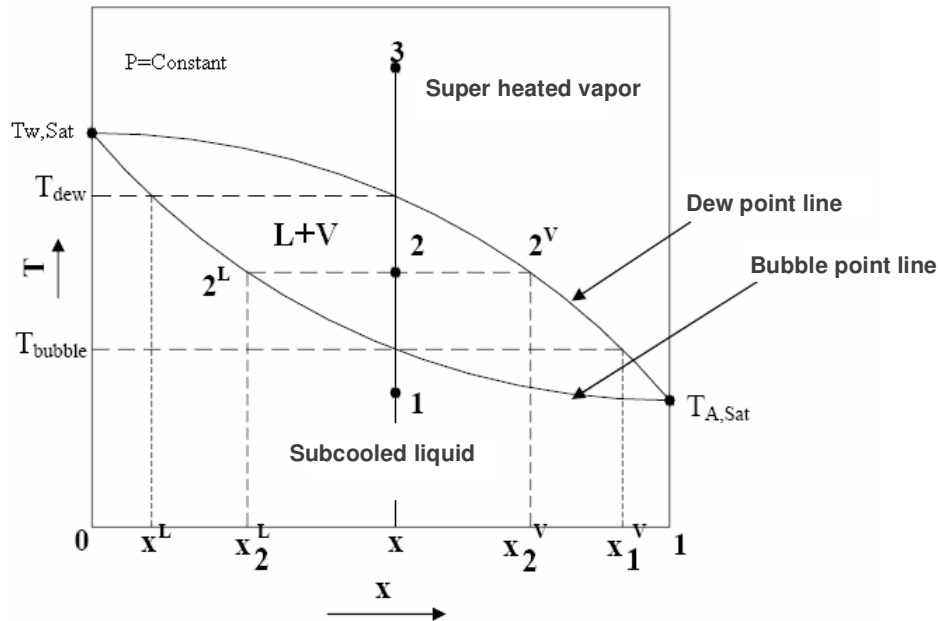*Corresponding author. E-mail: nshankar_g@rediffmail.com.

Figure 1. Equilibrium temperature-concentration curve for NH$_3$- H$_2$O at constant pressure.

time interval in obtaining the result. The presented work can be used for energy and exergy solutions to power generating systems. The exergy details and its concentration graph for the ammonia-water mixtures are not reported out in the literature, which is the gap identified and presented at various pressures.

THERMODYNAMIC EVALUATION OF NH$_3$-H$_2$O MIXTURE PROPERTIES

For ammonia-water mixture, to calculate the thermodynamic properties like specific enthalpy, specific entropy and specific volume, the need of bubble and dew point temperatures at various pressures and compositions are very essential and is the prior step. For estimating those temperatures, various correlations have been developed. The correlation developed by Patek and Klomfar (1995) is proposed in this work which avoids tedious iterations required by the complicated method fugacity coefficient of a component in a mixture and the correlation proposed by Ibrahim and Klein (1993).

Figure1 shows the details of bubble point and dew point temperature variations with ammonia concentration. The loci of all the bubble points are called the bubble point line and the loci of all the dew points are called the dew point line. The bubble point line is the saturated liquid line and the region between the bubble and dew point lines is the two phase region, where both liquid and vapor co-exist in equilibrium ("Vapor Absorption Refrigeration Systems Based on Ammonia-Water Pair", 2004).

Calculating bubble and dew point temperatures

The bubble point and dew point temperatures of the ammonia-water mixture are found from the correlations in Equations (1) and (2), developed by Patek and Klomfar (1995).

$$T_b\,(p, x) = T_o \sum_i a_i\,(1 - x)^{m_i} \left[\ln\!\left(\frac{p_o}{p}\right) \right]^{n_i} \tag{1}$$

$$T_d\,(p, y) = T_o \sum_i a_i\,(1 - y)^{m_i/4} \left[\ln\!\left(\frac{po}{p}\right) \right]^{n_i} \tag{2}$$

Figure 2 shows the bubble and dew point temperatures developed with the correlation by Patek and Klomfar (1995) up to pressure of 100 bar using MATLAB code. A flowchart was prepared to understand the mathematical calculations for properties.

Development of equations

The properties are derived from Gibbs free energy function from Ziegler and Trepp (1984).

Liquid phase

The Gibbs free energy for both liquid and gas phases were determined from Equations (3) and (4), developed by Ziegler and Trepp (1984) which is the summation of contributions of the pure components, the ideal free energy of mixing and the free excess energy.

$$g^l\,_{(T, p, x)} = \begin{Bmatrix} (1 - x)\,g^l_{H_2O}{}_{(T, p)} + x\,g^l_{NH_3}{}_{(T, p)} + \\ RT\big[(1 - x)\log_e(1 - x) + x\log_e x\big] + g_E{}_{(T, p, x)} \end{Bmatrix} \tag{3}$$
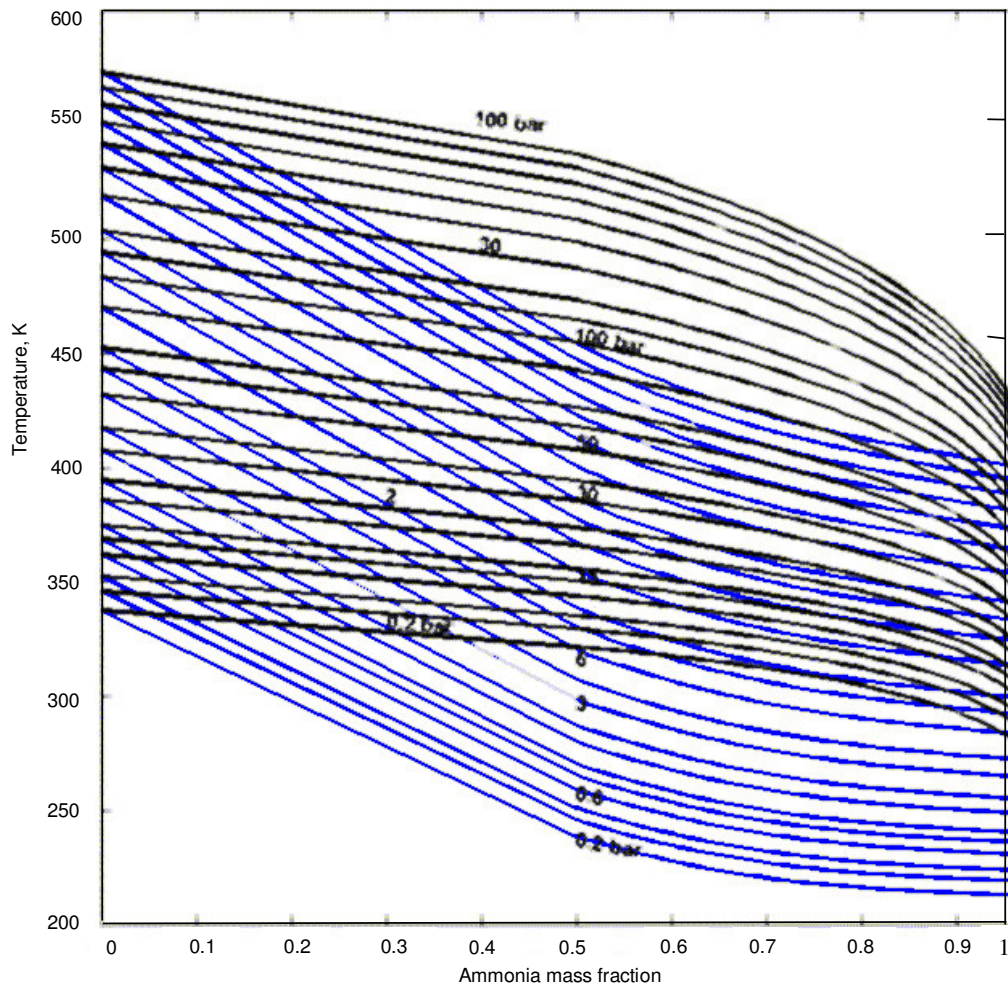
Figure 2. Bubble and dew point temperatures up to100 bar pressure.

Equation of state for pure component in liquid phase

The equation of state for pure components in liquid phase is given as follows:

$$g^l_{H_2O(T,p)} = \left[h^l(T_o,p_o) - Ts^l(T_o,p_o) + \int c_p^l dT - T \int \frac{c_p^l}{T} dT + \left(a_1 + a_3 T + a_4 T^2 \right)(p-p_o) + a_2 \frac{\left(p^2 - p_o^2 \right)}{2} \right]_{H_2O}$$

(4)

Where,

$$c^l_{p(T,p_o)} = b_1 + b_2 T + b_3 T^2$$

(5)

Similarly, the liquid heat capacity at constant pressure can be assumed to be second order in temperature according to Equation (5) (Ziegler and Trepp, 1984).On substituting (5) in Equation (4), the following Equations (6) and (7) were obtained for pure components in liquid phase.

$$g^l_{H_2O(T,p)} = \left\{ \left[h^l(T_o,p_o) - Ts^l(T_o,p_o) + \left[b_1(T-T_o) + \frac{b_2}{2}\left(T^2-T_o^2\right) + \frac{b_3}{3}\left(T^3-T_o^3\right) \right] \right] + \left[\left(a_1+a_3T+a_4T^2\right)(p-p_o) + a_2 \frac{\left(p^2-p_o^2\right)}{2} \right] \right\}_{H_2O}$$

(6)

$$g^l_{NH_3(T,p)} = \left\{ \left[h^l(T_o,p_o) - Ts^g(T_o,p_o) + \left[b_1(T-T_o) + \frac{b_2}{T}\left(T^2-T_o^2\right) + \frac{b_3}{3}\left(T^3-T_o^3\right) \right] \right] + \left[\left(a_1+a_3T+a_4T^2\right)(p-p_o) + a_2 \frac{\left(p^2-p_o^2\right)}{2} \right] \right\}_{NH_3}$$
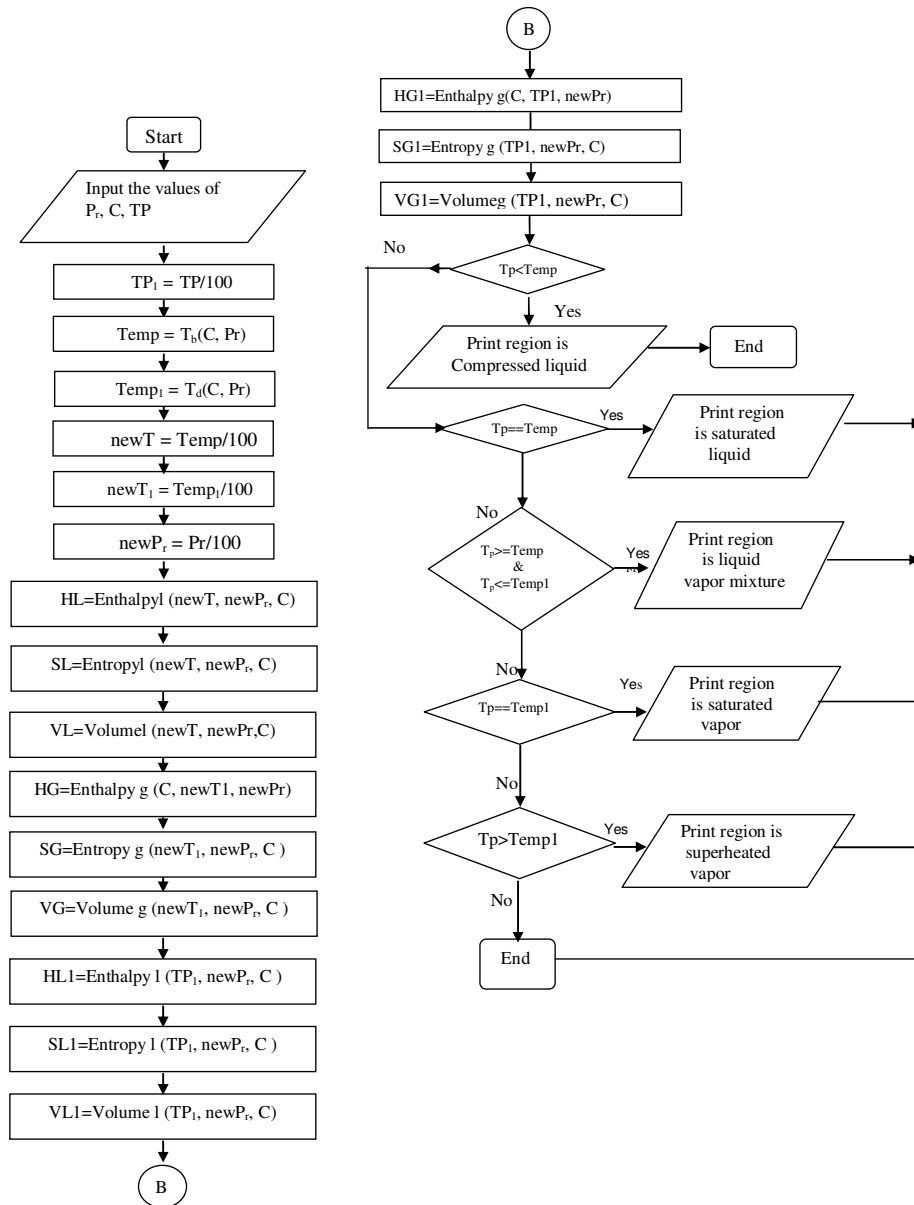
(7)

Figure 3. Flowchart to find thermodynamic properties of mixture.

Liquid mixture correlation

The Gibbs excess energy g_E for liquid mixtures is expressed as:

$$g_{E(T,p,x)} = \left\{ \begin{array}{l} \left(e_1 + e_2 p + (e_3 + e_4 p)T + \dfrac{e_5}{T} + \dfrac{e_6}{T^2} \right) + \\[2mm] (2x-1)\left(e_7 + e_8 p + (e_9 + e_{10}p)T + \dfrac{e_{11}}{T} + 3\dfrac{e_{12}}{T^2} \right) + \\[2mm] (2x-1)^2 \left(e_{13} + e_{14}p + \dfrac{e_{15}}{T} + \dfrac{e_{16}}{T^2} \right) \end{array} \right\}$$

(8)

In Figure 3, the procedure carried out in calculating the thermodynamic properties enthalpy, entropy and volume in both phases for the compressed region, saturated region, in between bubble and dew point region and superheated region were explained from the corresponding equations.

For a given pressure, concentration and temperature the bubble point and dew point temperatures were calculated and then the given temperature is compared with the bubble and dew temperatures and identifies the respective region as represented in the flowchart. The flowchart in Figure 3 shows the procedure for calculating the thermodynamic properties of the mixture. For a given property value, the corresponding regions can be identified from the flowchart.

Equation of state for pure component in gas phase

The general equation of state for pure component in gas phase is identified in the following equation.

$$g^g_{(T,P,Y)} = \left\{ \begin{array}{l} (1-y)g^g H_2 0_{(T,p)} + yg^g NH_{3(T,P)} + \\ RT\left[(1-y)\log_e(1-y) + y\log_e y\right] \end{array} \right\}$$

(9)

For the gas phase, the Gibbs free energy equation is given below:

$$g^g_{H_2O}(T,p) = \left\{ \begin{array}{l} h^g_{(T_o,p_o)} - Ts^g_{(T_o,p_o)} + \int C_p^{go} dT - T\int \frac{C_p^{go}}{T} dt + RT\ln\frac{p}{p_o} + c_1(p-p_o) + \\ c_2\left(\frac{p}{T^3} - 4\frac{p_o}{T_o^3} + 3\frac{p_oT}{T_o^4}\right) + c_3\left(\frac{p}{T^{11}} - 12\frac{p_o}{T_o^{11}} + 11\frac{p_oT}{T_o^{12}}\right) + \\ c_3\left(\frac{p}{T^{11}} - 12\frac{p_o}{T_o^{11}} + 11\frac{p_oT}{T_o^{12}}\right) + \frac{c_4}{3}\left(\frac{p^3}{T^{11}} - 12\frac{p_o^3}{T_o^{11}} + 11\frac{p_o^3T}{T_o^{12}}\right) \end{array} \right\}_{H_2O}$$

(10)

Where:

$$c_{p (T)}^{go} = d_1 + d_2 T + d_3 T^2$$

(11)

Similarly on substituting (11) in Equation (10), the pure components in gaseous phase from ammonia and water were obtained in Equations (12) and (13).

$$g^g_{H_2O}(T,p) = \left\{ \begin{array}{l} h^g_{(T_o,p_o)} - Ts^g_{(T_o,p_o)} + d_1(T_o-T) + \frac{d_2}{2}\left(T_o^2-T^2\right) + \frac{d_3}{3}\left(T_o^3-T^3\right) \\ + RT\log_e\frac{p}{p_o} + c_1(p-p_o) + c_2\left(\frac{p}{T^3} - 4\frac{p_o}{T_o^3} + 3\frac{p_oT}{T_o^4}\right) \\ + c_3\left(\frac{p}{T^{11}} - 12\frac{p_o}{T_o^{11}} + 11\frac{p_oT}{T_o^{12}}\right) + \frac{c_4}{3}\left(\frac{p^3}{T^{11}} - 12\frac{p_o^3}{T_o^{11}} + 11\frac{p_o^3T}{T_o^{12}}\right) \end{array} \right\}_{H_2O}$$

(12)

$$g^g NH_{3(T,p)} = \left\{ \begin{array}{l} h^g(T_o,p_o) - Ts^g(T_o,p_o) + d_1(T_o-T) + \\ \frac{d_2}{2}\left(T_o^2 - T^2\right) + \frac{d_3}{3}\left(T_o^3 - T^3\right) + \\ RT\log_e\frac{P}{P_o} + c_1(P-P_o) + \\ c_2\left(\frac{P}{T^3} - 4\frac{P^o}{T_o^3} + 3\frac{P_oT}{T_o^4}\right) \\ + c_3\left(\frac{P}{T^{11}} - 12\frac{P_o}{T_o^{11}} + 11\frac{P_oT}{T_o^{12}}\right) + \\ c_4\left(\frac{P^3}{T^{11}} - 12\frac{P_o^3}{T_o^{11}} + 11\frac{P_o^3T}{T_o^{12}}\right) \end{array} \right\}_{NH_3}$$

(13)

Equation of state for pure components

Specific enthalpy at liquid and vapor phases

The molar enthalpy of the liquid phase and gaseous phase were specified and simplified in Equation (14) to (19). Equation (16) is derived in MATLAB to find the liquid enthalpy in the compressed and saturated regions. Equation (19) is derived in MATLAB to find the enthalpy in gaseous phase for the saturated and superheated regions.

$$h^l = -RT_B T^2 \left(\frac{\partial\left(\frac{g^l(T,p,x)}{T}\right)}{\partial T} \right)_{p,x}$$

(14)

$$h^l = -RT_B T^2 \left\{ \begin{array}{l} (1-x)\frac{\partial}{\partial T}\left(\frac{g^l H_2 O_{T,p}}{T}\right) + \\ x\frac{\partial}{\partial T}\left(\frac{g^l NH_{3T,p}}{T}\right) \\ + \frac{\partial}{\partial T}R\left[(1-x)\log_e(1-x) + x\log_e x\right] \\ + \frac{\partial}{\partial T}\left(\frac{g^E(T,p,x)}{T}\right) \end{array} \right\}_{p,x}$$

(15)

$$h^l = \left\{ \begin{array}{l} \left(\frac{R}{18} \times T_B\right) \times (1-x) \times \left[\begin{array}{l} h^l(T_o, p_o) + b_1(T-T_o) + \frac{b_2}{2}\left(T^2-T_o^2\right) + \\ \frac{b_3}{3}\left(T^3-T_o^3\right) + \left(a_1 - a_4 T^2\right)(p-p_o) + \\ \frac{a_2}{2}\left(p^2-p_o^2\right) \end{array} \right]_{H_2O} + \\ \\ \left(\frac{R}{17} \times T_B\right) \times (x) \times \left[\begin{array}{l} h^l(T_o, p_o) + b_1(T-T_o) + \frac{b_2}{2}\left(T^2-T_o^2\right) + \\ \frac{b_3}{3}\left(T^3-T_o^3\right) + \left(a_1 - a_4 T^2\right)(p-p_o) + \\ \frac{a_2}{2}\left(p^2-p_o^2\right) \end{array} \right]_{NH_3} + \\ \\ \frac{R}{(x \times 17 + (1-x) \times 18)} \times T_B \times (x) \times (1-x) \times \left[\begin{array}{l} \left(e_1 + e_2 p + 2\frac{e_5}{T} + 3\frac{e_6}{T^2}\right) + \\ (2x-1)\left(e_7 + e_8 p + 2\frac{e_{11}}{T} + 3\frac{e_{12}}{T^2}\right) + \\ (2x-1)^2\left(e_{13} + e_{14}p + 2\frac{e_{15}}{T} + 3\frac{e_{16}}{T^2}\right) \end{array} \right] \end{array} \right\}$$

(16)

$$h^g = -RT_B T^2 \left(\frac{\partial \left(\frac{g^g_{(T,p,y)}}{T} \right)}{\partial T} \right)_{p,y}$$

(17)

$$h^g = -RT_B T^2 \left\{ (1-y)\frac{\partial}{\partial T}\left(\frac{g^g_{H_2O_{T,p}}}{T} \right) + y\frac{\partial}{\partial T}\left(\frac{g^g_{NH_{3_{T,p}}}}{T} \right) + \frac{\partial}{\partial T} R\left[(1-x)\log_e(1-x) + x\log_e x\right] \right\}_{p,y}$$

(18)

The subscript l indicates liquid
g indicates gas
o indicates ideal gas state
T_B = 100K
P_B = 10bar

$$h^g = \left\{ -\left(\frac{R}{18}\times T_B\right)\times(1-y)\times\left[h^g_{(To,po)} + d_1(T-T_o) + \frac{d_2}{2}\left(T^2-T_o^2\right) + \frac{d_3}{3}\left(T^3-T_o^3\right) + c_1(p-p_o) + 4c_2\left(\frac{p}{T^3}-\frac{p_o}{T_o^3}\right) + 12c_3\left(\frac{p}{T^{11}}-\frac{p_o}{T_o^{11}}\right) + 4c_4\left(\frac{p^3}{T^{11}}-\frac{p_o^3}{T_o^{11}}\right) \right]_{H_2O} \right.$$
$$\left. -\left(\frac{R}{17}\times T_B\right)\times y\times\left[h^g_{(To,po)} + d_1(T-T_o) + \frac{d_2}{2}\left(T^2-T_o^2\right) + \frac{d_3}{3}\left(T^3-T_o^3\right) + c_1(p-p_o) + 4c_2\left(\frac{p}{T^3}-\frac{p_o}{T_o^3}\right) + 12c_3\left(\frac{p}{T^{11}}-\frac{p_o}{T_o^{11}}\right) + 4c_4\left(\frac{p^3}{T^{11}}-\frac{p_o^3}{T_o^{11}}\right) \right]_{NH_3} \right\}$$

(19)

The coefficients used in Equations 15,17,20,23, 26 and 29 are given in (Table 1) and (Table 2).

Specific entropy at liquid and vapor phases

The molar entropy of the liquid and gaseous phases were specified and simplified in Equation (20) to (25). Equation (22) is derived in MATLAB to find the liquid entropy in the compressed and saturated regions. Equation (25) is derived in MATLAB to find the entropy in gaseous phase for the saturated and superheated regions.

$$s^l = -R\left(\frac{\partial g^l_{(T,p,x)}}{\partial T} \right)_{(p,x)}$$

(20)

$$s^l = -R\left\{ \frac{\partial}{\partial T}\left(\frac{(1-x)g^l_{H_2O_{(T,p)}} + x g^l_{NH_{3(T,p)}}}{+RT\left[(1-x)\log_e(1-x) + x\log_e x\right] + g_{E(T,p,x)}} \right) \right\}_{(p,x)}$$

(21)

On reduction, the above equation becomes:

$$s^l = \left\{ \begin{array}{l} \left[\frac{R}{18}\times(1-x)\left(s^l_{(To,po)} + b_1\log\left(\frac{T}{T_o}\right) + b_2(T-T_o) + \frac{b_3}{2}\left(T^2-T_o^2\right) + (-a_3-2a_4T)(p-p_o) \right)\right]_{H_2O} + \\ \left[\frac{R}{17}\times x\left(s^l_{(To,po)} + b_1\log\left(\frac{T}{T_o}\right) + b_2(T-T_o) + \frac{b_3}{2}\left(T^2-T_o^2\right) + (-a_3-2a_4T)(p-p_o) \right)\right]_{NH_3} - \\ \left[\frac{R}{x.17+(1-x).18}\times\frac{R}{x.17+(1-x).18}\times\left((1-x)\log_e(1-x) + x\log_e x\right) + \frac{R}{x.17+(1-x).18}\times x\times(1-x)\left(se_1+se_2+se_3\right)\right] \end{array} \right\}$$

(22)

Where:

$$se_1 = -e_3 - e_4 p + \frac{e_5}{T^2} + \frac{2e_6}{T^3}$$

$$se_2 = (2x-1)\left(-e_9 - e_{10}p + \frac{e_{11}}{T^2} + \frac{2e_{12}}{T^3} \right)$$

$$se_3 = (2x-1)^2\left(\frac{e_{15}}{T^2} + \frac{2e_{16}}{T^3} \right)$$

$$s^g = -R\left(\frac{\partial g^g_{(T,p,y)}}{\partial T} \right)_{(p,y)}$$

(23)

$$s^g = -R\left\{ \frac{\partial}{\partial T}\left(\frac{(1-y)g^g_{H_2O_{(T,p)}} + y g^g_{NH_{3(T,p)}}}{+RT\left[(1-y)\log_e(1-y) + y\log_e y\right] + g_{E(T,p,y)}} \right) \right\}_{(p,y)}$$

(24)

$$s^g = \left\{ \begin{array}{l} \left[-\frac{R}{18}\times(1-y)\left(-s^g_{(To,po)} - d_1\log\left(\frac{T}{T_o}\right) + \frac{d_2}{2}(2T_o-2T) + \frac{d_3}{2}\left(T_o^2-T^2\right) + \frac{R}{18}\log\left(\frac{p}{po}\right) + c_2\left(\frac{3p_o}{T_o^4}-\frac{3p}{T^4}\right) + c_3\left(\frac{11p_o}{T_o^{12}}-\frac{11p}{T^{12}}\right) + \frac{c_4}{3}\left(\frac{11p_o^3}{T_o^{12}}-\frac{11p^3}{T^{12}}\right) \right)\right]_{H_2O} + \\ \left[-\frac{R}{17}\times(y)\left(-s^g_{(To,po)} - d_1\log_e\left(\frac{T}{T_o}\right) + \frac{d_2}{2}(2T_o-2T) + \frac{d_3}{2}\left(T_o^2-T^2\right) + \frac{R}{18}\log_e\left(\frac{p}{po}\right) + c_2\left(\frac{3p_o}{T_o^4}-\frac{3p}{T^4}\right) + c_3\left(\frac{11p_o}{T_o^{12}}-\frac{11p}{T^{12}}\right) + \frac{c_4}{3}\left(\frac{11p_o^3}{T_o^{12}}-\frac{11p^3}{T^{12}}\right) \right)\right]_{NH_3} - \\ \left[-\left(\frac{R}{y.17+(1-y).18}\times\frac{R}{y.17+(1-y).18}\right)\times\left((1-y)\log_e(1-y) + y\log_e y\right)\right] \end{array} \right\}$$

(25)

Table 1. Coefficients for the equations for the pure components.

Coefficient	Ammonia	water
a_1	$3.971423.10^{-2}$	$2.748796.10^{-2}$
a_2	$-1.790557.10^{-5}$	$-1.016665.10^{-5}$
a_3	$-1.308905.10^{-2}$	$-4.452025.10^{-3}$
a_4	$3.752836.10^{-3}$	$8.389246.10^{-4}$
b_1	$1.634519.10^{1}$	$1.214557.10^{1}$
b_2	-6.508119	-1.898065
b_3	1.448937	$2.911966.10^{-1}$
c_1	$-1.049377.10^{-2}$	$2.136131.10^{-2}$
c_2	-8.288224	$-3.169291.10^{1}$
c_3	$-6.647257.10^{2}$	$-4.634611.10^{4}$
c_4	$-3.045352.10^{3}$	0.0
d_1	3.673647	4.019170
d_2	$9.989629.10^{-2}$	$-5.175550.10^{-2}$
d_3	$3.617622.10^{-2}$	$1.951939.10^{-2}$
h^l	4.878573	21.821141
h^g	26.468879	60.965058
s^l	1.644773	5.733498
s^g	8.339026	13.453430
T_o	3.2252	5.0705
p_o	2.0000	3.0000

Table 2. Coefficients for the Gibbs excess energy function.

e_1	$-4.626129.10^{1}$
e_2	$2.060225.10^{-2}$
e_3	7.292369
e_4	$-1.032613.10^{-2}$
e_5	$8.074824.10^{1}$
e_6	$-8.461214.10^{1}$
e_7	$2.452882.10^{1}$
e_8	$9.598767.10^{-3}$
e_9	-1.475383
e_{10}	$-5.038107.10^{-3}$
e_{11}	$-9.640398.10^{1}$
e_{12}	$1.226973.10^{2}$
e_{13}	-7.582637
e_{14}	$6.012445.10^{-4}$
e_{15}	$5.487018.10^{1}$
e_{16}	$-7.667596.10^{1}$

Specific volume of liquid and vapor phases

The specific volume of the liquid and gaseous phases, were specified and simplified in Equation (26) to (31). Equation (28) is derived in MATLAB to find the liquid volume in the compressed and saturated regions. Equation (31) is derived in MATLAB to find the volume in gaseous phase for the saturated and superheated regions.

$$v^l = \frac{RT_B}{p_B}\left(\frac{\partial}{\partial p}g^l{}_{(T,p,x)}\right)_{(T,x)}$$

(26)

$$v^l = \frac{RT_B}{p_B}\left\{ \begin{array}{l} (1-x)\left(\frac{\partial}{\partial P}g^l{}_{H_2O}\right)_{T,p,x} + (x)\left(\frac{\partial}{\partial P}g^l{}_{NH_3}\right)_{T,p,x} + \\ \frac{\partial}{\partial P}RT[(1-x)\log_e(1-x)+x\log_e x] + \frac{\partial}{\partial P}g_E{}_{T,p,x} \end{array} \right\}_{T,x}$$

(27)

In the same manner specific volumes were solved.

$$v^l = \left\{ \begin{array}{l} \left(\frac{R}{18}\times\frac{T_B}{100p_B}\times(1-x)\times(a_1+a_2p+a_3T+a_4T^2)\right)_{H_2O} + \\ \left(\frac{R}{17}\times\frac{T_B}{100p_B}\times(x)\times(a_1+a_2p+a_3T+a_4T^2)\right)_{NH_3} + \\ \frac{R}{x.17+(1-x).18}\times\frac{T_B}{100p_B}\times x(1-x)\times(e_2+e_4T+(2x-1)e_8+e_{10}T+(2x-1)^2e_{14}) \end{array} \right\}$$

(28)

$$v^g = \frac{RT_B}{p_B}\left(\frac{\partial}{\partial p}g^g{}_{(T,p,y)}\right)_{(T,y)}$$

(29)

$$v^g = \left[\frac{RT_B}{p_B}\left\{ \begin{array}{l} (1-y)\left(\frac{\partial}{\partial P}g^g{}_{H_2O}\right)_{T,p,y} + (y)\left(\frac{\partial}{\partial P}g^g{}_{NH_3}\right)_{T,p,y} + \\ \frac{\partial}{\partial P}RT[(1-y)\log_e(1-y)+y\log_e y] \end{array} \right\}_{T,y} \right]$$

(30)

$$v^g = \left\{ \begin{array}{l} \left(\frac{R}{18}\times\frac{T_B}{100p_B}\times(1-y)\times\left(\frac{R}{18}\times\frac{T}{p}\right)+c_1+\frac{c_2}{T^3}+\frac{c_3}{T^{11}}+\frac{c_4p^2}{T^{11}}\right)_{H_2O} + \\ \left(\frac{R}{17}\times\frac{T_B}{100p_B}\times y\times\left(\frac{R}{18}\times\frac{T}{p}\right)+c_1+\frac{c_2}{T^3}+\frac{c_3}{T^{11}}+\frac{c_4p^2}{T^{11}}\right)_{NH_3} \end{array} \right\}$$

(31)

RESULTS AND DISCUSSION

In this study, from the simplified Equations 17 and 19 the liquid and vapor enthalpies were calculated and coded in MatLab. Similarly, Equations 22 and 25 were used to calculate the liquid and vapor entropies. The results generated using these equations were programmed in MatLab. With MatLab, the graphs were plotted and compared with the graphs from the Feng and Yogi (1999). The graphs obtained from this work, show a very close trend of comparison, Feng and Yogi (1999).
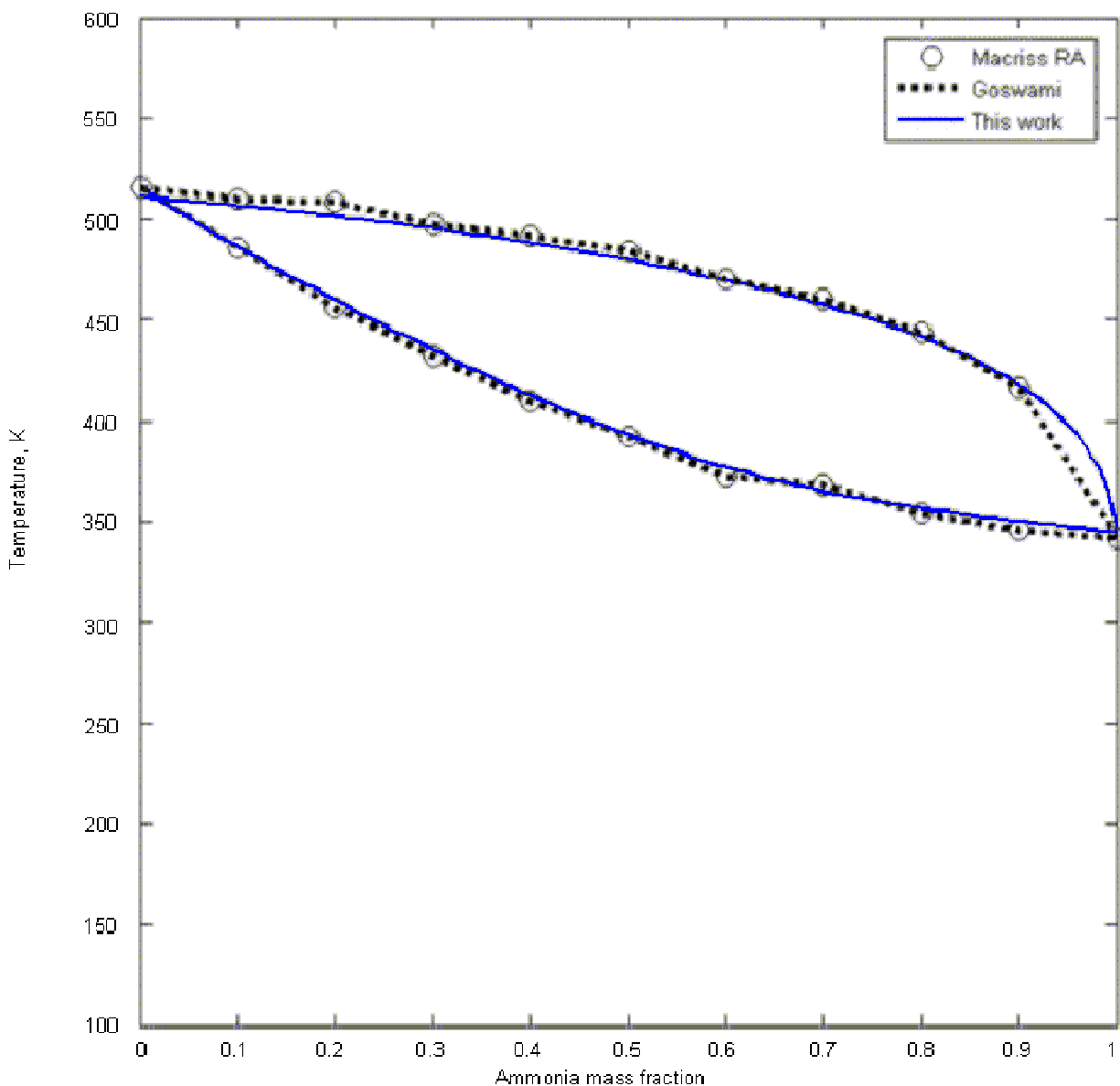
Figure 4. Bubble and dew point temperatures a 34.47 bar.

Figure 4 shows a plot between the temperature and ammonia mass fraction. Here, the data in the sense of the values of temperature at a particular concentration. The temperatures at a particular concentration obtained from Macriss and Goswami (1999) are very close with the produced result using MatLab. Figure 4 shows the bubble point temperature and dew point temperature curves at a specified pressure and for different concentrations. The bubble point temperature and dew point temperature values are identical at initial and final concentrations ensuring a closed curve. The differences between our computed values and the data are less than 0.5%.The simulated works were carried out in MATLAB, which

shows a closer match with the literature. This work requires less calculation and can be utilized for the thermodynamic properties.

(Table 3) gives the property values at different regions. For a given pressure, temperature and concentration the bubble and dew point temperatures were calculated and the given temperature will be compared with those two temperatures and determine in which region the given temperature lies. If the given temperature is less than the bubble point temperature then region will be a compressed liquid region and for which the corresponding enthalpy, entropy and volumes were obtained using MATLAB. In calculating the dryness

Table 3. Thermodynamic properties value at different regions (p = 65 bar, x = 0.6, T = 125 °C, T_b = 138 °C and T_d = 228 °C).

T °C	Condition	h_l kJ/kg	h_g kJ/kg	h kJ/kg	s_l kJ/kg-K	s_g kJ/kg-K	s kJ/kg-K	v_l m³/kg	v_g m³/kg	V m³/kg
125	Compressed liquid	366.68	-	-	1.40	-	-	0.0015	-	-
138	Saturated liquid curve	435.95	-	-	1.57	-	-	0.0016	-	-
215	Two phase region-	-	-	1775.94	-	-	4.59	-	-	0.008
228	Saturated vapor curve	-	1978.23	-	-	5.04	-	-	0.011	-
250	Superheated	-	2049.47	-	-	5.18	-	-	0.012	-

fraction, the ammonia mole fraction of vapor phase is obtained from correlation by Soleimani (2007).

$$y(x,P) = 1- \exp[aP^b x + (c +d /P) x^2] \qquad (32)$$

The present results found a closer match with the existing results in the plots at a temperature less than 500 °C and 100 bar. In finding the values of enthalpy, entropy and volume in between Tb and Td regions the dryness fraction is calculated from the equation developed in (19).

The liquid enthalpy and vapor enthalpy plots were shown in (Figure 5) and (Figure 6). From (Figure 5), the variation in the liquid enthalpy decreases first and then increases with increase in concentration at a specified pressure. The results obtained were validated and shows a closer match with the compared results. The differences are less than 3% for all the data. (Figure 6) shows the variation in the vapor enthalpy curve. The enthalpy value decreases continuously with the increase in the concentration. The enthalpy concentration with respect to the parameters pressure and concentration is shown in (Figure 7). The liquid enthalpy plot is obtained by considering the bubble point temperature and ammonia mole fraction of liquid phase. For plotting the auxiliary curve the liquid enthalpy is considered as a function of bubble point temperature and ammonia mole fraction of vapor phase. (Figure 7) of the present work has got similar curves at saturated liquid and vapor conditions as compared with existing graph by Ziegler and Trepp (1984). The values of enthalpies at any concentration and pressure from the result (22) is compared with the present values and got similar values. The ammonia mole fraction of vapor phase is obtained by correlation by Soleimani (2007). With the utilization of these correlations the result shows good agreement with the previous work. With the combination of correlations stated in the abstract, the present work was carried out using a new program code MatLab and shows the similar trends in all the graphs. Work is the properties from the combination of the three correlations and obtained in MatLab. (Figure 8) shows the entropy of saturated liquid at a specified temperature and various concentrations.

(Figure 8) shows the entropy of saturated liquid at a

specified temperature and various concentrations. The entropy decreases and increases with the increase in concentration. The plot obtained is validated with the existing results and produces a good match. Whereas in the entropy of saturated vapor from (Figure 9) at a specified temperature, the plot decreases continuously with the increase in concentration. (Figure 10) shows the entropy concentration diagram for ammonia - water mixture at various pressures and concentrations. The gap on the left hand side between the liquid curves is less compared with the gap on the right side of the plot which can even be extended to 150 bar with the same correlations. The values obtained by this plot can be utilized for any thermodynamic cycle. Upon increasing the pressures vapor curve and auxiliary curve are embedded one over the other forming a close gap between each other.

Figures (11 and 12) shows the liquid volume and vapor volume which has been derived utilizing bubble point temperature. With both the plots at a specified pressure the volume decreases with the increase in concentration. Exergy analysis is the maximum useful work obtained during an interaction of a system with equilibrium state. The total exergy of a system becomes a summation of physical exergy and chemical exergy.

$$E = E_{ch} + E_{ph} \qquad (33)$$

$$E_{ph} = (h-h_o)-T_o(s-s_o) \qquad (34)$$

$$E_{ch} = \left[\frac{x_i}{M_{NH_3}}\right] e^o_{ch , NH_3} + \left[\frac{(1 - x_i)}{M_{H_2O}}\right] e^o_{ch , H_2O}$$

$$\qquad (35)$$

Where e^o_{ch}, NH_3 and e^o_{ch}, H_2O are chemical exergies o ammonia and water. The standard chemical exergy of ammonia and water are taken from Ahrendts (1980).

The exergy concentration plot for ammonia-water mixture at various pressures is shown in (Figure 13). The liquid exergy curve decreases to certain concentration and approaches a near constant relation. The vapor exergy
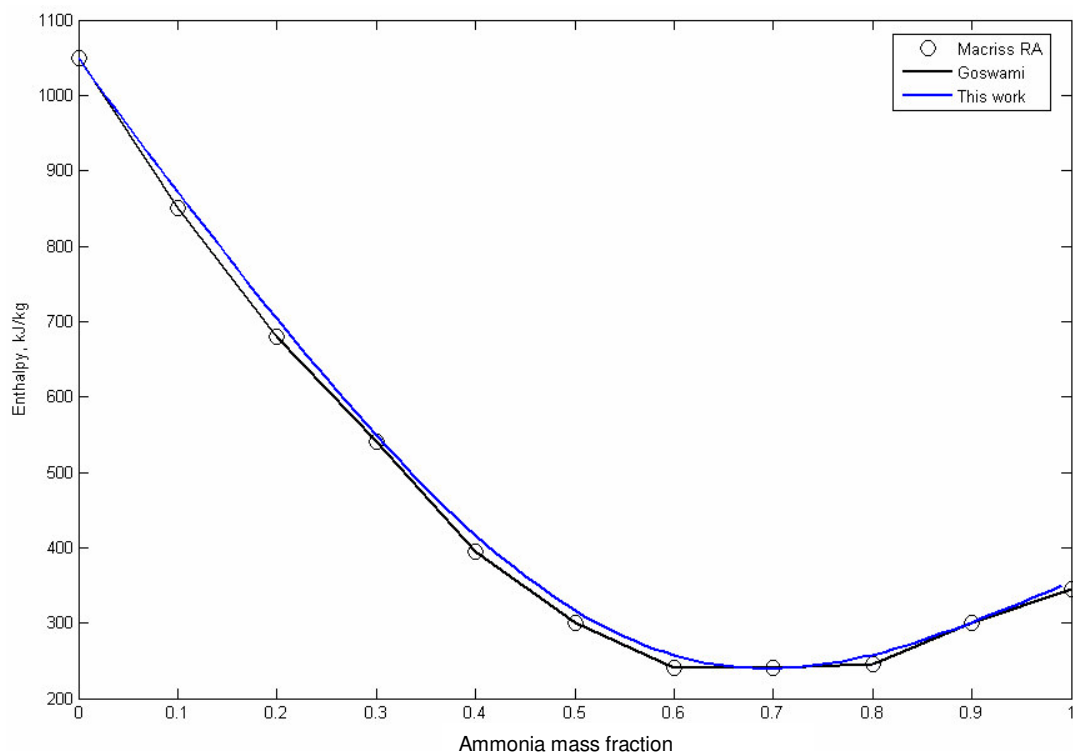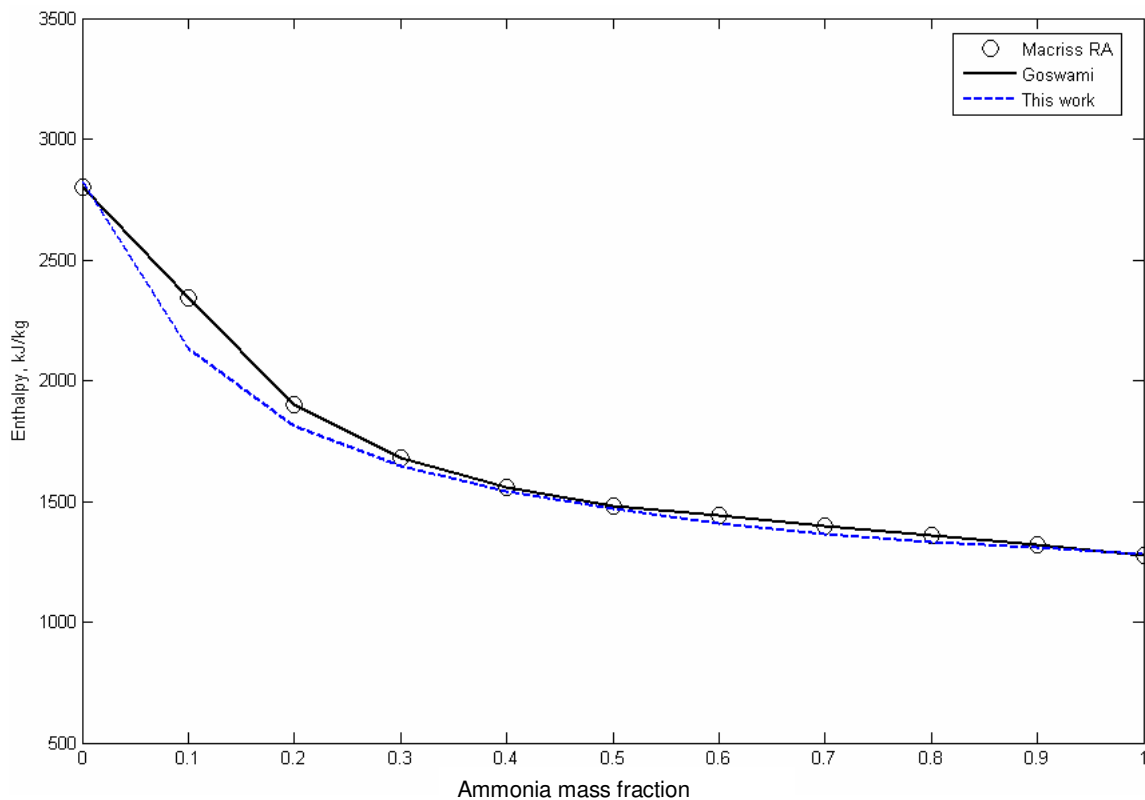
Figure 5. Enthalpy of saturated liquid at P=34.47 bar.
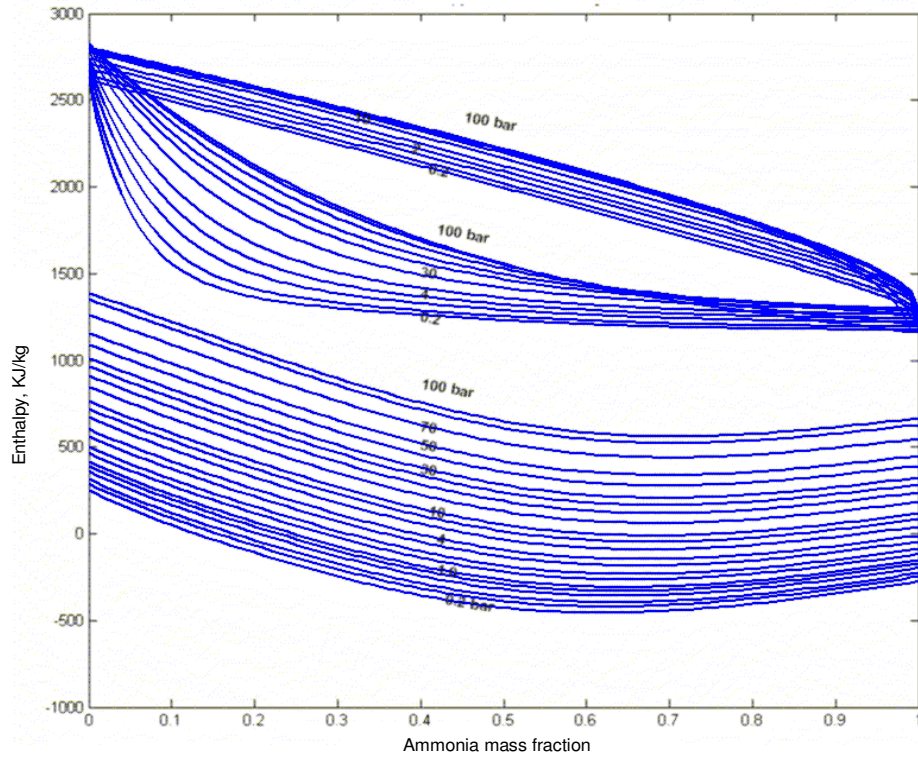

Figure 6. Enthalpy of saturated vapor at 34.47 bars.
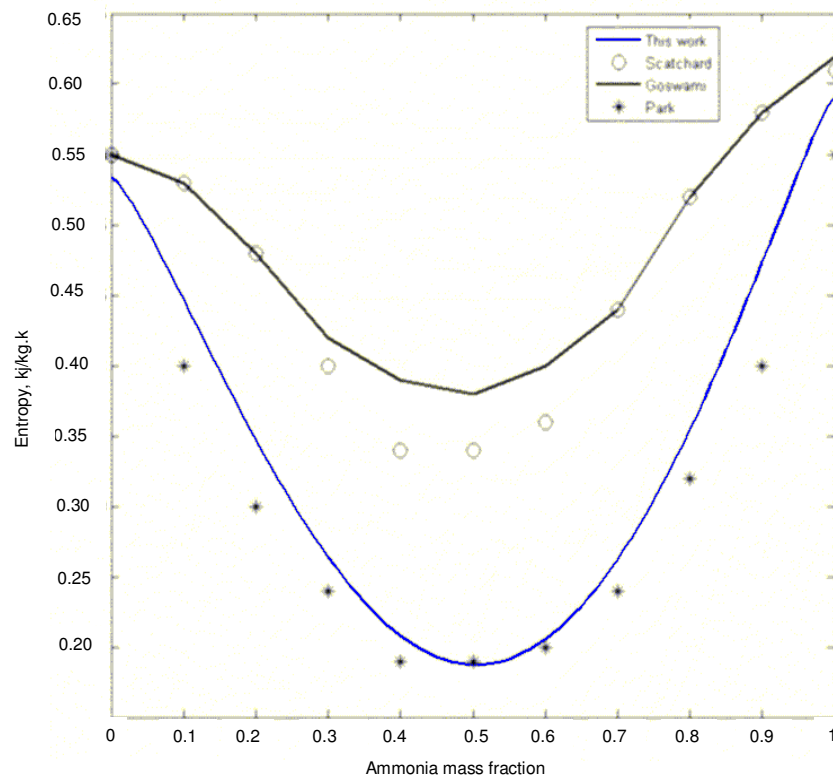
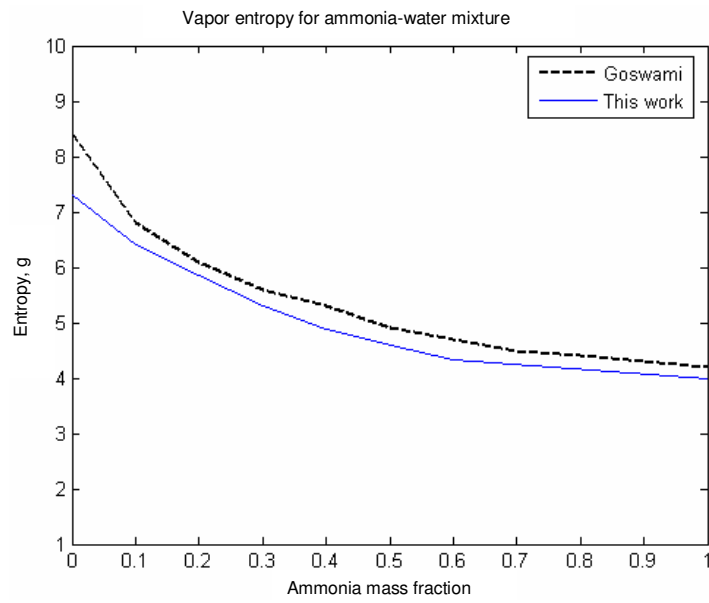**Figure 7.** Ammonia-water enthalpy concentration diagram.

Figure 8. Entropy of saturated liquid at 37 °C.
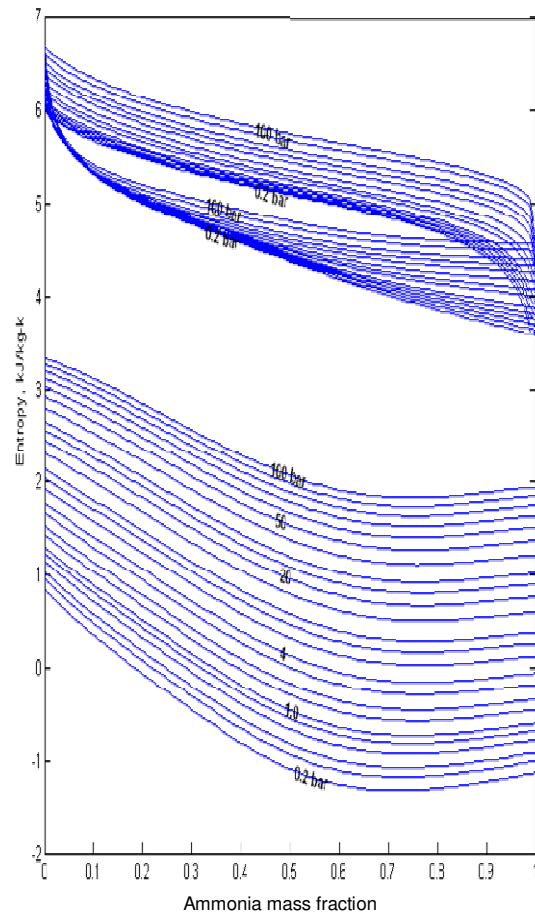
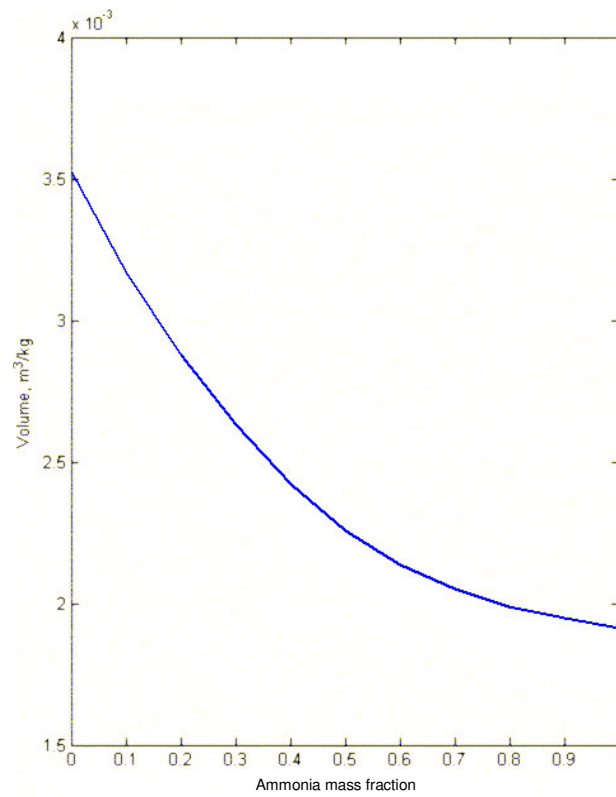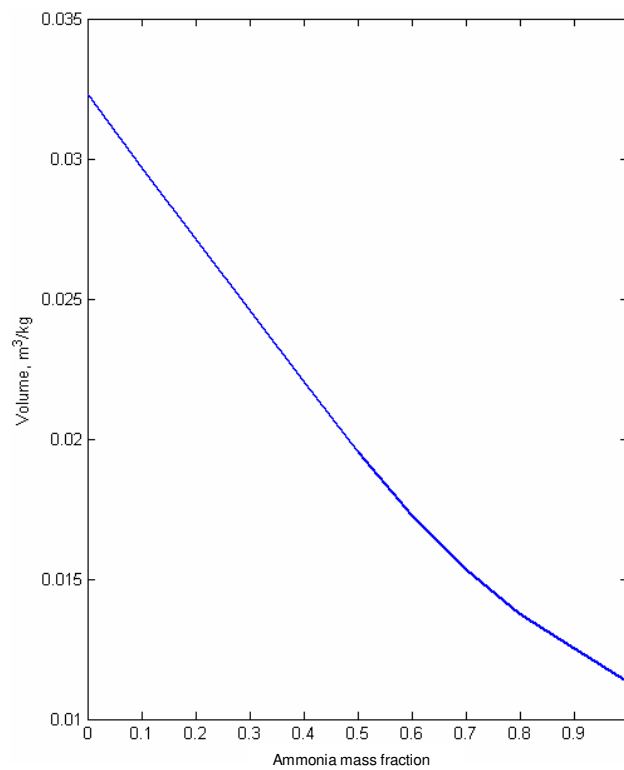**Figure 9.** Entropy of saturated vapor at 37 °C.
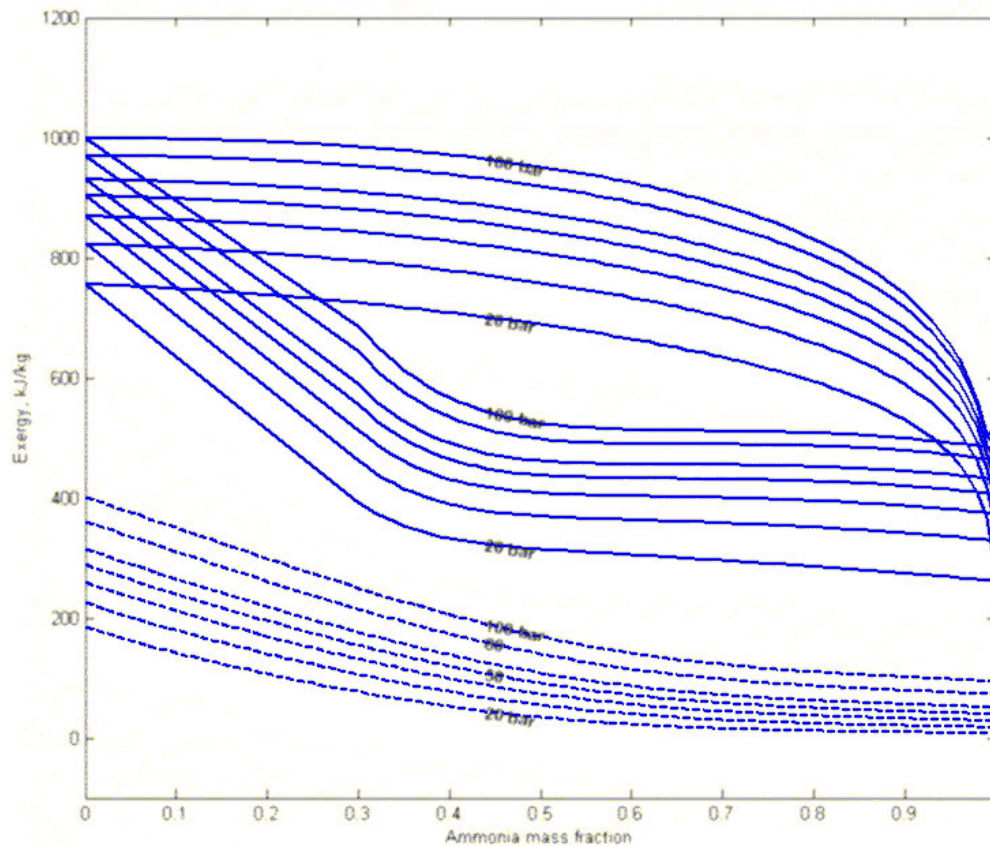

Figure 10. Entropy concentration diagram for ammonia-water mixture.

Figure 11. Volume of saturated liquid at P=34.47 bar.

Figure 12. Volume of saturated vapor at P=34.47 bar.

Figure 13. Exergy concentration diagram for ammonia-water mixture.

curve decreases continuously with the increase in concentration. The gap on the left hand side between the liquid curves is wider than the right hand side. The auxiliary lines are contracting at low ammonia fractions whereas the same lines are expanding at high ammonia fractions. The vapor exergy curve and auxiliary curves have identical values at initial and final concentrations which results in a closed loop. The space between the liquid exergy and the closed loop is reduced with the increase in pressures.

Conclusion

To develop thermodynamic properties of ammonia-water mixtures various correlations were analyzed. In this work three different correlations were utilized for developing the results. Bubble and dew point temperatures were obtained utilizing the correlation of Patek and Klomfar (1995), which reduces iterations, which is been utilized for finding the properties enthalpy, entropy and volume. The properties were derived using relations Ziegler and Trepp (1984). The mole fraction of ammonia in vapor phase was solved with the correlation by Soleimani

(2007). With the utility of these correlations, the need of tedious iterations used in fugacity method was reduced. The results obtained in this work were validated by comparing with the published data and found closer matching. Here, the results of the graphs obtained from MatLab are compared with the existing results and proves the similar trends, which is the evidence and that is why it was mentioned, as found to have close match. The exergy for the ammonia-water system have been simulated with the help of the derived properties, to carry out the second law analysis to power systems.

Nomenclature: a_i, b_i, c_i, d_i, e_i, m_i, n_i, ρ, Coefficients; **h,** specific enthalpy, kJ/kg; **s,** specific entropy, kJ/kg-K; **v,** specific volume, m^3/kmol; **T,** temperature, K; p, pressure, bar; **g,** Gibbs free energy, kJ/kmol; **c_p,** specific heat capacity at constant pressure, kJ/kmol-K; **R,** universal gas constant, kJ/kmol-K; **x,** ammonia mole fraction in liquid phase; **y,** ammonia mole fraction in vapor phase.

Superscripts: g, Gas phase; **l,** liquid phase; **o,** ideal gas state.

Subscripts: b, Bubble point; **d,** dew point; **o,** reference state.

REFERENCES

Ahrendts J (1980). Reference states , Energy, 5: 667-668.

Abovsky V (1996). "Thermodynamics of ammonia-water mixture", Fluid Phase Equilibria, 116: 170-176.

Barhoumi M, Snoussi A, Ben EN, Mejbri K, Bellagi A (2004). "Modeling of the thermodynamic properties of the ammonia/water mixture. Int. J. Refrig., 27: 271-283.

Feng X, Yogi GD (1999). "Thermodynamic properties of ammonia-water mixtures for power-cycle applications" Energy, 24: 525-536.

Hasan O, Stanley I, Sandler (1995). "On the combination of equation ofstate and excess free energy models", Fluid Phase Equilibria, 111: 53-70.

Ibrahim OM, Klein SA, (1993). "Thermodynamic Properies of ammonia-water mixture", ASHRAE Trans., 99: 1495-1502

Eric W, Lemmon, Reiner T (1999). "A Helmholtz energy equation of state for calculating the thermodynamic properties of fluid mixtures", Fluid Phase Equlibria, 165: 1-21.

Mejbri KH, Bellagi A (2006). "Modelling of the thermodynamic properties of the water-ammonia mixture by three different approaches, Int. J. Refrig., 29: 211-218.

Mishra RD, Sahoo PK, Gupta A (2006). "Thermoeconomic evaluation and optimization of an aqua-ammonia vapour-absorption refrig. system" Int. J. Refrig., 29: 47-59.

Nowarski A, Friend DG (1998). "Application of the extended corresponding states method to the calculation of the ammonia-water mixture thermodynamic surface", Int. J. Thermophys., 19: 1133-1141.

Patek J, Klomfar J (1995). "Simple functions for fast calculations of selected thermodynamic properties of the ammonia-water system", Refrig., 18: 228-234.

Reid RC, Prausnitz JM, Poling BE (1987). The Properties of Gases and Liquids. Fourth edition. New York, USA: McGraw-Hill. 667. ISBN 0-07-051799-1.

Renon H, Guillevic JL, Richon D, Boston J, Britt H (1985). "A cubic equation of state representation of ammonia-water vapor-liquid equilibrium data" Refrig., 9: 70-73.

Ruiter JP (1990). "Simplified thermodynamic description of mixtures and solutions", 13: 223-236.

Raj S, Diwakar S, Ranjana G, Ashish D (1999). "Potential applications of artificial neural networks to thermodynamics: Vapor-liquid equilibrium predictions, Comput. Chem. Eng., 23: 385-390.

Senthil R, Murugan PMV, Subbarao(2008) "Thermodynamic Analysis of Rankine-Kalina Combined Cycle", Int. J. Thermodyn., 11: 133-141.

Soleimani G, Alamdari (2007). "Simple functions for predicting the thermodynamic properties of ammonia-water mixture", 20(1): 95-104.

Tillner-Roth R, Friend DG (1998). "A Helmholz free energy formulation of the thermodynamic properties of the mixture, American Institute of Physics and American Chemical Society.

"Vapor Absorption Refrigeration Systems Based on Ammonia-Water Pair" (2004). Version 1. ME, IIT.

Weber LA, (1999). "Estimating the virial coefficients of the ammonia-water mixture" Fluid Phase Equlibria, 162: 31-49

Yousef SH, Najjar (1997). "Determination of thermodynamic properties of some engineering fluids using two-consant equations of state, Thermochim. Acta, 303: 137-143.

Ziegler B, Trepp CH (1984). "Equation of state for ammonia-water mixtures" Refrig., 7: 101-106.